DEVELOPMENT AND DISEASE

The *heartstrings* mutation in zebrafish causes heart/fin Tbx5 deficiency syndrome

Deborah M. Garrity, Sarah Childs* and Mark C. Fishman[†]

Cardiovascular Research Center, Massachusetts General Hospital, 149 13th Street, Charlestown, MA 02129, USA
*Present address: Department of Biochemistry and Molecular Biology, Faculty of Medicine, University of Calgary, Calgary AB, Canada, T2N 4N1
[†]Author for correspondence (e-mail: mcfishman@partners.org)

SUMMARY

Holt-Oram syndrome is one of the autosomal dominant human 'heart-hand' disorders, with a combination of upper limb malformations and cardiac defects. Holt-Oram syndrome is caused by mutations in the *TBX5* gene, a member of a large family of T-box transcription factors that play important roles in cell-type specification and morphogenesis. In a screen for mutations affecting zebrafish cardiac function, we isolated the recessive lethal mutant *heartstrings*, which lacks pectoral fins and exhibits severe cardiac dysfunction, beginning with a slow heart rate and progressing to a stretched, non-functional heart.

We mapped and cloned the *heartstrings* mutation and find it to encode the zebrafish ortholog of the *TBX5* gene. The *heartstrings* mutation causes premature termination at amino acid 316. Homozygous mutant embryos never develop pectoral fin buds and do not express several markers of early fin differentiation. The total absence of any fin bud differentiation distinguishes *heartstrings* from most other mutations that affect zebrafish fin development,

suggesting that Tbx5 functions very early in the pectoral fin induction pathway. Moderate reduction of Tbx5 by morpholino causes fin malformations, revealing an additional early requirement for Tbx5 in coordinating the axes of fin outgrowth. The heart of *heartstrings* mutant embryos appears to form and function normally through the early heart tube stage, manifesting only a slight bradycardia compared with wild-type siblings. However, the heart fails to loop and then progressively deteriorates, a process affecting the ventricle as well as the atrium.

Relative to mammals, fish require lower levels of Tbx5 to produce malformed appendages and display whole-heart rather than atrial-predominant cardiac defects. However, the syndromic deficiencies of *tbx5* mutation are remarkably well retained between fish and mammals.

Key words: Holt-Oram syndrome, Zebrafish, T-box, Tbx5, Heart, Pectoral fin, Limb induction

INTRODUCTION

Members of the T-box family of transcription factors contain a highly conserved DNA binding motif of 180-190 amino acid residues (Murray, 2001; Simon, 1999; Tada and Smith, 2001). T-box genes are represented throughout metazoan evolution, and vertebrates alone include over 20 family members (Tada and Smith, 2001). T-box genes play key roles in cell-type specification and morphogenesis (Smith, 1999), and mutations in several T-box genes have been shown to result in human developmental disorders (Murray, 2001). For example, mutations in *TBX5* cause human Holt-Oram syndrome, characterized by congenital defects in the heart and upper limbs (Basson et al., 1997; Li et al., 1997). *TBX3* mutations produce ulnar-mammary syndrome (Bamshad et al., 1997; Bamshad et al., 1999). Mutations in *TBX22* cause the rare syndrome CPX (X-linked cleft palate and tongue-tie) (Braybrook et al., 2001). Mutations in *TBX1* are responsible

for the DiGeorge syndrome (Lindsay et al., 2001; Merscher et al., 2001).

The function of *tbx5* in the heart appears to be exquisitely sensitive to gene dosage, since either haploinsufficiency or gene duplication can produce the cardiac abnormalities associated with Holt-Oram syndrome (Dixon et al., 1993; Hatcher and Basson, 2001; McCorquodale et al., 1986; Melnyk et al., 1981). The sensitivity to dose may be explained in part by the synergistic interaction of Tbx5 with other transcription factors, including Nkx2.5 (Bruneau et al., 2001; Hiroi et al., 2001), and its activation or co-activation of multiple downstream targets including *connexin40* and *atrial natriuretic factor* (Bruneau et al., 2001; Ghosh et al., 2001; Hiroi et al., 2001). Although *tbx5* is expressed early in the cardiogenic mesoderm prior to heart tube formation (Bruneau et al., 1999; Chapman et al., 1996; Horb and Thomsen, 1999; Liberatore et al., 2000), specific functions in heart field specification have not been identified. Several *tbx* genes may play overlapping

functions in early decisions of cardiac cell fate, as suggested by complete elimination of cardiac tissue by dominant negative effects of *tbx5-engrailed* constructs injected into *Xenopus* embryos (Horb and Thomsen, 1999). The earliest described phenotypic effects in mice with a targeted mutation in *tbx5* (*Tbx5*^{−/−} mice) include hypoplasia of the inflow tract, atria, and to a lesser extent, the left ventricle (Bruneau et al., 2001). Dominant effects observed in heterozygous human or *Tbx5*^{+/−} mice include atrial and ventricular septal defects, and electrophysiological defects, particularly atrioventricular block (Bruneau et al., 2001; Newbury-Ecob et al., 1996).

tbx5 is expressed in a dynamic pattern in the developing heart tube. At early stages, human (Hatcher et al., 2000a; Li et al., 1997), mouse (Bruneau et al., 1999; Chapman et al., 1996; Christoffels et al., 2000; Liberatore et al., 2000), chicken (Bruneau et al., 1999; Liberatore et al., 2000) and frog (Horb and Thomsen, 1999) show somewhat different patterns of *tbx5* expression, but by completion of cardiac looping all express *tbx5* in a posterior-to-anterior gradient with highest levels of expression in the atria and absence of expression in the conotruncus or outflow tract. *tbx5* is expressed in the heart of zebrafish (Begemann and Ingham, 2000; Ruvinsky et al., 2000), but its anteroposterior expression pattern was not described. Anteroposterior localization appears to be important, because engineered persistent expression of mouse *tbx5* in the entire heart tube perturbs chamber-specific gene expression and retards ventricular chamber morphogenesis (Liberatore et al., 2000).

Tbx5 also plays a role in the developing limb (Simon, 1999; Tamura et al., 2001). *tbx5* is expressed in the forelimb, and *tbx4* in the hindlimb, suggesting that *tbx5* controls forelimb identity, and *tbx4* hindlimb identity (Gibson-Brown et al., 1998; Isaac et al., 1998; Logan et al., 1998; Ohuchi et al., 1998). Ectopic expression of Tbx5 or Tbx4 in chick partially transforms the identity of developing limbs, in accordance with this suggestion (Logan and Tabin, 1999; Rodriguez-Esteban et al., 1999; Takeuchi et al., 1999). The skeletal defects observed in patients with Holt-Oram syndrome, or experimentally, in limbs produced from ectopic buds in chick, indicate that Tbx5 also coordinates later limb outgrowth. Limb deformities in the Holt-Oram syndrome range from mild thumb deformities to a near absence of the arm (phocomelia) (Basson et al., 1994; Newbury-Ecob et al., 1996).

We here report the isolation of a recessive mutation that affects heart and pectoral fin formation in the zebrafish embryo. The pectoral fin is homologous to the tetrapod forelimb (Tamura et al., 2001). *heartstrings* (*hst*) is an unusual mutation in that even the earliest molecular evidence of pectoral fin bud generation is absent. The heart in *hst* mutant embryos forms relatively normally, but deteriorates during looping and later stages. We positionally cloned the *hst* locus, and show it encodes the zebrafish ortholog of *tbx5*. The *hst* mutation appears to eliminate Tbx5 function entirely, but we find Tbx5 function is markedly dose-dependent, especially in fin bud formation.

MATERIALS AND METHODS

Zebrafish lines

We identified the *hst*[m21] mutation in a screen for ENU-induced mutations on a TL background, as described previously (Chen et al., 2001). We maintained mutations by outcrossing to standard wild-type lines (WIK and TL). Embryos were raised and staged as described previously (Kimmel et al., 1995).

Meiotic and physical mapping of *hst*

We mapped the *hst* locus to the telomere of linkage group 5 using bulked segregant analysis (Michelmore et al., 1991) on a panel of 120 microsatellite markers from the zebrafish genetic map (Knapik et al., 1998). DNA of homozygous *hst*[m21] embryos (4974 meioses) was tested against individual microsatellite markers (Z markers) to refine the critical interval. BAC clones were identified by screening DNA pools by PCR (Incyte Genomics). We used the QIAGEN plasmid Midi kit to extract BAC DNA. We obtained BAC end sequences by direct sequencing (MWG Biotech). Simple sequence repeats (SSRs), single nucleotide polymorphisms (SNPs) or simple sequence length polymorphisms (SSCPs) were defined in BAC end sequences and used to develop genetic markers for fine mapping. Genetic and physical maps were coordinated using the Goodfellow radiation hybrid (RH) panel (Geisler et al., 1999).

Identification of the *hst* mutation

RNA was extracted from wild-type or homozygous *hst* embryos aged 48 hours post-fertilization (hpf). RT-PCR of the *tbx5* gene was performed using the Promega Access kit and primers tbxF4 (TTTTGGTTGTTTAGGGATTCG) and tbxR2 (AGCACAATG-TTTGCTGCTTC), followed by nested PCR with primers tbxF3 (GGAATTTAAGGCCTCACGGTA) and tbxR3 (TGATGTGT-CCAGTGCTCCTT). PCR products of four independent RNA samples were sequenced on both strands and aligned using the MacVector gene analysis program.

In situ hybridization, antibody, skeletal staining and histology

Whole-mount in situ hybridization and antibody staining was carried out as described previously (Thisse et al., 1993). Antibodies were obtained from Dr Frank Stockdale (MF-20 and S46). For skeletal stains, whole pectoral fins were excised from adults and fixed overnight in 4% paraformaldehyde. Alcian Blue/Alizarin Red staining was performed as described previously (Grandel and Schulte-Merker, 1998). For sectioning, embryos were mounted in JB-4 plastic medium (Polysciences), sectioned at 5 µm, stained with Methylene Blue/Fuchsin (Grandel and Schulte-Merker, 1998) and photographed with a Zeiss Axioscope.

Morpholino treatment

The morpholino antisense oligonucleotide "tbx-MO" (5′ GAAAG-GTGTCTTCACTGTCCGCCAT 3′) was designed against the *tbx5* translational start site and purchased from Gene Tools, LLC. Wild-type or *hst* embryos primarily at the 1-cell stage with chorion intact were injected with ~2 nl of stocks ranging from 750 to 100 µM (12.4 to 1.7 ng) of morpholino diluted in Danieau's solution.

RESULTS

hst is required for heart growth and pectoral fin induction

We identified the ENU-induced allele *heartstrings*[m21] (*hst*) in a large-scale screen for recessive lethal mutations that perturb cardiac function. Homozygous *hst* mutant embryos have severe cardiac and pectoral fin abnormalities, and die between 6 and 7 days post-fertilization (dpf). Heterozygous *hst* embryos have normal anatomy, and adults are viable and fertile.

The morphology of the initial heart tube of *hst* mutant

Table 1. Comparison of heart rate in *hst* and wild-type embryos

Embryo age	*hst*	Wild type	% of wild type
25 hpf	65.19±12.00	76.77±10.32	84.92
48 hpf	116.43±12.66	150.03±15.21	77.60
72 hpf	110±24.03	172.68±16.20	64.03

Values are beats per minute ± standard deviation. At least 45 embryos were scored for every timepoint. *hst* and wild type values are significant ($P<0.001$) at every timepoint.

embryos at 24-26 hpf is indistinguishable from wild type. Both atrium and ventricle are evident and contract normally. The one subtle difference from wild type is heart rate. From the onset of cardiac contraction, hearts of *hst* mutant embryos beat slower than those of their wild-type siblings (Table 1). Measurements of heart rate (beats/minute) at 25 hpf, the earliest time-point at which regular heart rates could be scored, indicate the heart rate of *hst* mutant embryos is approximately 84.9% of wild-type siblings. By 2 dpf, the heart rate of *hst* mutant embryos is 77.6% of the wild-type siblings. Heart rates of heterozygote embryos are not different from wild type.

The first morphological defect in hearts of *hst* mutant embryos is failure to complete looping. The atrium completes the first step of situs formation (Chen et al., 1997), jogging to the left at 24 hpf. Thereafter, *hst* hearts remain central and linear (Fig. 1A,B). Circulation is vigorous in *hst* mutant embryos through 2 dpf. However, shortly thereafter *hst* hearts slowly stretch to a thin, 'string-like' morphology and circulation ceases by 3 or 4 dpf (Fig. 1C-E), as contractility progressively decreases. Pericardial edema is present at 2 dpf and frequently massive by 3 dpf (Fig. 1E). The extent of pericardial edema and degree of heart stretching varies with different WIK genetic backgrounds (Fig. 1D,E).

hst mutant embryos do not develop pectoral fins. Moreover, in contrast to nearly all zebrafish pectoral fin mutants described to date (Allende et al., 1996; Barresi et al., 2000; Begemann and Ingham, 2000; Begemann et al., 2001), *hst* mutant embryos do not produce any morphologically recognizable fin buds (Fig. 1F,G). In wild-type fins outgrowth begins around 26 hpf as mesodermal cells of the fin field assume a perpendicular arrangement with respect to the basement membrane of the epidermis, begin to proliferate, and push the overlying epidermis outward (Grandel and Schulte-Merker, 1998; van Eeden et al., 1996; Yelon et al., 2000). Small buds are apparent by 28 hpf. As buds grow out, the initially unstructured epidermal layer develops into the apical fold, analogous to the tetrapod apical ectodermal ridge (AER) (Neumann et al., 1999). In cross-sections of 48 hpf *hst* embryos, we observe small bilateral patches of dark-staining somatopleure mesodermal cells in the area from which wild-type buds emanate (Fig. 2A,B). By 3 dpf, these mesenchymal cells occasionally assume an orientation perpendicular to the basement membrane, but they do not proliferate further (Fig. 2C). No buds are evident in *hst* embryos examined up to day 6 (Fig. 1H,I), indicating that bud growth is not simply delayed.

The *hst* locus encodes the T-box transcription factor Tbx5

We identified the *hst* gene by positional cloning. We mapped the *hst* mutant locus to the telomere of LG5, between Z10827
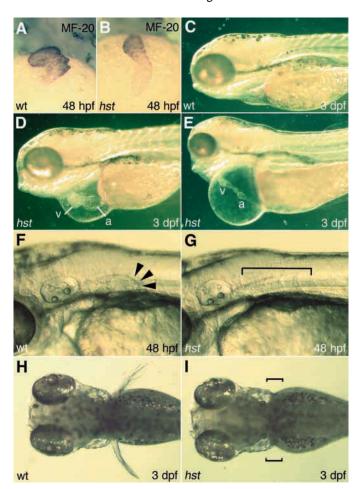

Fig. 1. Cardiac and pectoral fin abnormalities in *hst* mutant embryos. (A,C,F,H) Wild-type embryos; (B,D,E,G,I,J) *hst* mutant siblings. (A,B) Immunostaining with the cardiac-specific antibody MF-20 at 48 hfp in hearts of embryos near completion of looping (ventral views, anterior towards top). (C-I) Live embryos. (C-E) 3 dpf. *hst* mutant embryos (D,E) have mild to severe pericardial edema and an unlooped, stretched heart. (F,G) 48 hpf. (F) Wild-type embryos display pectoral fin buds with apical fold (arrowheads). (G) Pectoral fin buds are missing in *hst* mutant embryos (bracket). (H,I) 3 dpf. (H) Wild-type pectoral fins elongate, but (I) *hst* mutant embryos have still not developed fin buds (brackets). (C-G) Lateral views; (H,I) dorsal views. a, atrium, v, ventricle.

and Z22208, and generated a physical contig bridging these two Z markers (Fig. 3A). Polymorphism in BAC-end sequences provided a means of generating SNP and SSCP markers subsequently used to map recombinants. Analysis of 4974 meiosis narrowed the critical interval to 0.08 cM (Fig. 3A). The *tbx5* gene (AF185283) mapped within 2 cRad of the *hst* locus on the Goodfellow RH panel. *tbx5* was an excellent candidate for *hst*, since mutations in human *TBX5* result in congenital heart defects accompanied by malformations of the forelimb. We sequenced *tbx5* cDNA generated by RT-PCR in *hst*[m21] mutant embryos, and found a C to T transition at base pair 1356, which converts a glutamine to a premature stop codon (Q316Stop; Fig. 3B,C). The glutamine residue 316 is conserved in humans, chick, mouse and newts, but is not a site of previously described mutations.

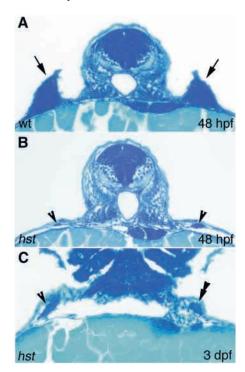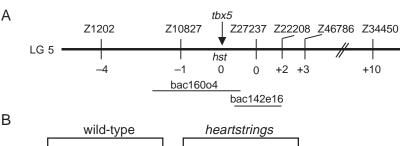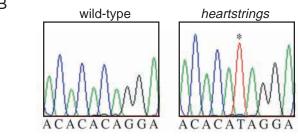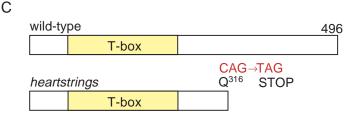The *hst* mutation lies approximately two-thirds of the way

Fig. 2. Arrested pectoral fin bud induction in *hst* mutant embryos. (A,B) Methylene Blue-stained cross sections through 48 hpf embryos. (A) Wild-type embryos have pectoral fin buds (arrows). (B) *hst* mutant embryos retain small populations of presumptive fin mesenchymal cells (arrowheads) that fail to proliferate. (C) Methylene Blue-stained transverse sections of 3 dpf mutant embryos. Presumptive fin mesenchyme is usually present as a flat patch (arrowhead), but occasionally cells turn perpendicular to the basement membrane (double arrowhead), but do not proliferate further.

into the *tbx5* open reading frame (Fig. 3C). If translated, the predicted mutant protein would contain the complete T-box binding domain and a portion of the carboxy-terminal region. The T-box domain of *tbx5* modulates its DNA binding and protein dimerization activities, while the carboxyl-terminal region contains elements that positively regulate binding (Hiroi et al., 2001).

Mutant proteins that retain the ability to dimerize or to bind DNA without concomitant trans-activation have the potential to exert dominant negative activity (Veitia, 2002). Indeed, carboxy-terminal truncations in the T-box protein Brachyury with dominant negative activity have been described (Herrmann, 1991). However, we do not have genetic evidence for dominant effects of the *hst* mutation, and *hst* heterozygotes are phenotypically indistinguishable from wild-type embryos. The number of mutant offspring from *hst* heterozygote incrosses is 25.8% (379/1396).

Premature nonsense codons can destabilize the transcripts leading to nonsense mediated decay (Nagy and Maquat, 1998). However, *hst* transcripts are expressed in mutant embryos by in situ hybridization at levels comparable to wild type, suggesting that RNA stability is not markedly reduced by the mutation.

Morpholino-mediated translational inhibition of Tbx5 phenocopies *hst*

To examine whether *hst* defects are due to loss of Tbx5 function, we reduced Tbx5 levels by injection of morpholino-modified antisense oligonucleotides. Morpholinos inhibit the translation of specific RNA target molecules and have been shown to phenocopy a number of early zebrafish mutations (Heasman, 2002). We used a morpholino directed against the *tbx5* translational start site (tbx5-MO), and find injection of 12.4 ng produces a progression of heart and limb defects indistinguishable from those in *hst* mutant embryos in 93% (272/292) of injected embryos (Fig. 4). At 25 hpf, the mean heart rate of morphant-injected embryos is 82.6% of uninjected embryos (*n*=43 morphants, 44 uninjected controls), a rate similar to *hst* embryos of the same age (Table 1). This progresses to failure of looping and cardiac dysfunction with a string-like heart. Fin buds do not form. We observed a milder version of the *hst* phenotype (see below) in 2.1% (6/292) of injected embryos. 5.1% (15/292) of embryos displayed defects in trunk and tail development, or necrosis in the CNS, common non-specific defects noted with injection of other morpholinos delivered at high

Fig. 3. Cloning and mapping of zebrafish *hst*. (A) An integrated genetic and radiation hybrid (RH) panel map of the telomere of linkage group 5 (LG5), showing selected CA-repeat 'Z' markers, and the number of recombinant events detected from 4974 meioses. The position of *tbx5* on the RH panel coincides with the critical genetic interval defined by linkage mapping of the *hst* locus. (B) Sequencing of the *tbx5* cDNA reveals a C to T change at base pair 1356 in *hst* mutant embryos. This mutation changes residue 316 (glutamine) to a premature stop codon. (C) A schematic of the *tbx5* cDNA indicating the extent of the T-box domain and the location of the *hst* stop codon.

dose (Ekker and Larson, 2001; Imai and Talbot, 2001). Lower doses of tbx5-MO (1.7 ng), phenocopy the mutation in 64% (76/118) of embryos, and cause a milder version with slight cardiac dysfunction, little or no pericardial edema, and undersized, delayed pectoral fin buds (Fig. 4E,H) in 30% (33/118) of embryos. Similar effects of *tbx5* morpholinos on pectoral fin development were recently described by Ahn et al. (Ahn et al., 2002).

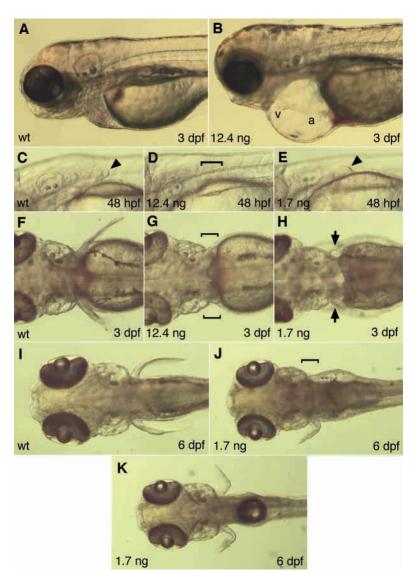The phenocopy produced by tbx5-MO is not more severe than the *hst* phenotype, suggesting that *hst*[m21] is a strong allele, possibly null. To test this further, we injected tbx5-MO into offspring from two heterozygous *hst* parents. Tbx5-MO injection does not enhance the phenotype further in homozygous *hst* mutant embryos. Moreover, a low dose of tbx5-MO (1.7 ng) is sufficient to "convert" *hst* heterozygotes to a homozygous mutant phenotype, suggesting that *hst* mutation exerts its effects by affecting gene dose via loss-of-function rather than dominant-negative mechanisms.

tbx5 expression pattern in the heart and fin buds

tbx5 expression in the heart of *hst* mutant embryos is identical to wild type, when analyzed by RNA in situ hybridization. *tbx5* transcripts appear as bilateral stripes in the lateral plate mesoderm (LPM) beginning at the 6- or 7-somite stage (Begemann and Ingham, 2000; Ruvinsky et al., 2000; Tamura et al., 1999; Yelon et al., 2000). The domain of *tbx5* expression expands mediolaterally between the 10- and 15-somite stage. Thereafter, anterior (heart-forming) regions migrate medially, whereas the posterior (fin-forming) regions remain broadly spread across the yolk. At the 20-somite stage, when the heart tube is first assembled as a cone, *tbx5* is expressed in the myocardial precursors as well as bilaterally in broad posterior regions that constrict by 26 hpf to form roughly circular fin fields.

Patterns of *tbx5* expression in the heart differ among species, and have not previously been described in detail beyond 30 hpf in the zebrafish (Begemann and Ingham, 2000; Ruvinsky et al., 2000). At 26 hpf, expression in the presumptive
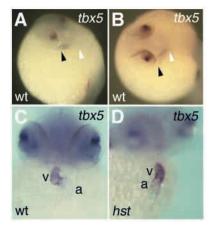

Fig. 4. Translational inhibition by *tbx5* morpholino. (A-K) Live embryos; (A,C,F,I) wild-type embryos; (B,D,G) embryos injected with 12.4 ng *tbx5* morpholino (tbx5-MO); (E,H,J,K) embryos injected with 1.7 ng tbx5-MO. (A,B) Injection of 12.4 ng of tbx5-MO phenocopies heart stretching and pericardial edema of *hst* mutant embryos, and (C,D) eliminates bud formation at 48 hpf. (E) Injection of 1.7 ng of tbx5-MO delays the onset of bud formation to shortly before 48 hpf. (F,G) 12.4 ng tbx5-MO continues to inhibit bud formation at 3 dpf. (H) Buds of 1.7 ng-injected embryos grow slowly. (I-K) 6 dpf embryos. (I) Wild-type buds elongate to a growing fin. (J,K) 1.7 ng-injected embryos in which the initial buds develop into shorter up-turned fins. (J) Some embryos develop only one bud and hence one fin. (A-E) Lateral views; (F-K) dorsal views. a, atrium; v, ventricle; arrowheads, developing pectoral fin buds; brackets, regions where fin bud failed to develop.

Fig. 5. *tbx5* expression in the heart tube. (A,B) In situ hybridization of 26 hfp embryos. (A) At 26 hpf, *tbx5* expression is detectable first in the presumptive atrium. (B) Upon longer exposure to substrate, *tbx5* expression extends through presumptive atrium and ventricle. Heart tubes of wild-type (shown) and *hst* mutant embryos (not shown) look identical at this stage. (C,D) In situ hybridization of 48 hfp embryos. (C, wild type; D, *hst*) *tbx5* expression is strongest in the ventricle, and weaker in the atrium. a, atrium; v, ventricle; black arrowhead, venous (atrial) end of heart tube; white arrowhead, arterial (ventricular) end of heart tube.

atrium is slightly greater than in the presumptive ventricle (Fig. 5A,B). *tbx5* expression in the heart tube of *hst* mutant embryos is identical to wild type at this and later stages, despite incomplete looping in *hst* mutant embryos. An atrial-enhanced pattern of *tbx5* expression is noted in other species (Bruneau et al., 1999; Chapman et al., 1996; Christoffels et al., 2000; Hatcher et al., 2000b; Horb and Thomsen, 1999; Li et al., 1997; Liberatore et al., 2000). Surprisingly, in zebrafish the *tbx5* expression gradient reverses in direction by 48 hpf, when looping is almost complete (Fig. 5C,D). At 48 hpf and beyond, *tbx5* expression is strongest in the ventricle, weaker in the atrium, and absent in the inflow tract (Fig. 5C,D). We do not detect *tbx5* expression in the outflow tract at any time. Thus, the pattern of *tbx5* expression in the heart at later stages has polarity opposite to that of other vertebrate species.

Late onset cardiac deterioration in *hst* mutant embryos

hst mutant embryos show normal expression of *nkx2.5, hand2, bmp4, cmcl2* and *vhmc* in the cardiac precursor regions at the 15-somite stage (Fig. 6). All of these markers are present in broad bilateral bands in the LPM, and show normal anteroposterior localization. These results suggest the heart field is properly demarcated and myocardial specification occurs normally in the *hst* mutant embryos.

In other species, *tbx5* appears to play an important role in the assignment of atrial and ventricular cell fates in the heart (Bruneau et al., 2001; Liberatore et al., 2000). In zebrafish, atrial and ventricular lineages can be distinguished with molecular markers well before the chambers become morphologically discrete (Yelon et al., 1999; Yelon and Stainier, 1999). The presumptive ventricle expresses

Fig. 6. Early cardiac markers are normal in *hst* mutant embryos at the 15-somite stage. Dual in situ hybridization using: (A) *nkx2.5/ntl*, (B) *hand2/ntl*, (C) *bmp4/ntl*, (D) *cmcl2/ntl*, (E) *vhmc/ntl*, (F) *ntl* alone. The *ntl* probe indicates the anterior extent of the notochord (arrow in F) (Serbedzija et al., 1998).

ventricular myosin heavy chain (*vmhc*) (Yelon et al., 1999), while the presumptive atrium expresses an atrial-specific myosin heavy chain recognized by the S46 antibody (Stainier and Fishman, 1992). Both *vmhc* and S46 are expressed

Fig. 7. Myocardial differentiation in *hst* mutant embryos. (A-D) In situ hybridization with the ventricle-specific marker *vmhc* (purple) followed by immunohistochemistry with the atrial-specific S46 antibody (brown). (A, wild type; B, *hst*) *vmhc*/S46 expression was normal at 33 hpf and (C, wild type; D, *hst*) at 48 hpf. (E-H) *versican* expression in the heart. At 33 hpf (not shown), wild-type and *hst* mutant embryos express *versican* broadly in the atrium and weakly in the ventricle. (E,F) 48 hpf; (G,H), 72 hpf; (E,G) wild-type embryos restrict *versican* expression to the AV boundary, but (F,H) *hst* mutant embryos fail to undergo this transition and continue to express *versican* predominantly in the atrium, with weak expression in the ventricle. (I-L) *bmp4* expression in the heart. (I) Wild-type and (J) *hst* mutant embryos express *bmp4* in the ventricle and inflow tract at 48 hpf. By 72 hpf (K) wild-type embryos restrict *bmp4* to the AV junction, but (L) *hst* mutant embryos retain ventricle-enriched expression. (M-P) *versican* expression in the developing ear. At 48 hpf, (M) wild-type and (N) *hst* mutant embryos express *versican* broadly in the otic placode. By 72 hpf, (O) wild-type and (P) *hst* mutant embryos both restrict *versican* to the otoliths (Mowbray et al., 2001), suggesting the heart-specific defects in *hst* mutant embryos are not due to general developmental delay. a, atrium; av, atrioventricular boundary; i, inflow tract; op, otic placode; ot, otoliths; pf, pectoral fin bud; v, ventricle.
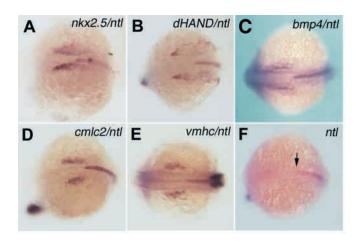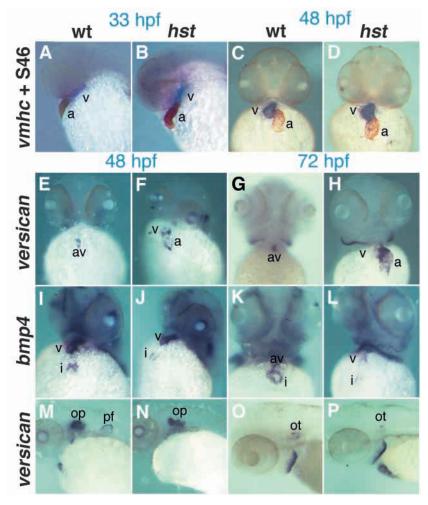
normally in the heart in *hst* mutant embryos at 26 and 48 hpf (before and after overt chamber formation; Fig. 7A-D). These data suggest that atrial and ventricular fates are assigned properly in *hst* mutant embryos. Similarly, the atrial-enriched expression of *versican* (Thisse et al., 1993; Walsh and Stainier, 2001) and ventricle-enriched expression of *bmp4* are relatively normal in the *hst* mutant embryos at 33 hpf (data not shown). However, shortly thereafter progression of differentiation appears to arrest in hearts of *hst* mutant embryos. The normal retraction of *versican* expression to the atrioventricular boundary after 37 hpf, and of *bmp4* expression to the same region after 48 hpf, does not occur in *hst* mutant embryos (Fig. 7E-L). Beginning around this stage there is progressive diminution of contractility and evident deterioration of the heart in embryos homozygous for the *hst* mutation. In mice mutant for *tbx5*, the sinoatrial structures and primitive left ventricle are severely hypoplastic (Bruneau et al., 2001). Interestingly, the early deterioration of the heart in *hst* mutant embryos does not greatly perturb the morphology of the inflow tract, but the atrium and ventricle are both affected. The atrium becomes stretched and can eventually rip open. The ventricle is smaller, with less concentric growth, and is only weakly contractile (Fig. 8A,B).

The pectoral fin field fails to differentiate in *hst* mutant embryos

We examined the stage at which the *tbx5* mutation perturbs fin development. Normally, between the 10- and 15-somite stages, LPM fin field precursors spread mediolaterally (Yelon et al., 2000). *tbx5* expression, present in the LPM from the 7-somite stage onward, becomes restricted to a dorsal patch coincident with the presumptive fin field by 26 hpf. *tbx5* expression continues in the mesenchyme of the outgrowing fin bud from 48 hpf (Fig. 9A-C) through 5 dpf (Begemann and Ingham, 2000). In *hst* mutant embryos, the pattern of *tbx5* expression in the LPM is normal up to the 20-somite stage. At 26 hpf, when fin bud outgrowth would normally initiate, *tbx5* expression in the posterior LPM fails to condense into a circular patch and levels of transcript decrease greatly (Fig. 9A′). We detect only a few *tbx5*-positive cells by 32 hpf (Fig. 9B′), and no expression in the pectoral fin-forming region of the LPM at 48 hpf (Fig. 9C′).
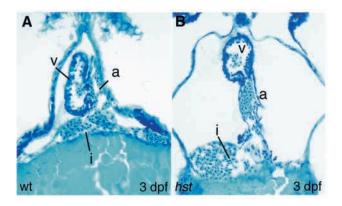
From 28 hpf, wild-type embryos express *shh* in the posterior mesenchyme (the ZPA; Fig. 9D) (Krauss et al., 1993; Neumann et al., 1999; Sordino et al., 1995), and *dlx2* and *bmp4* in the
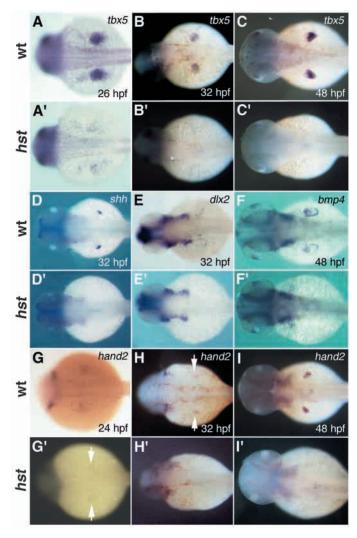

Fig. 9. Fin bud development in *hst* mutant embryos. (A-I) Wild-type embryos, (A′-I′) *hst* mutant embryos. (A-C′) *tbx5* expression in the developing pectoral fin field. At 26 hpf, (A) wild-type embryos restrict *tbx5* expression to a circular patch, the presumptive fin field, in the dorsal LPM, but (A′) *hst* mutant embryos display a more dispersed, less abundant expression. (B,B′) At 32 hpf and (C,C′) at 48 hpf, (B,C) wild-type embryos continue *tbx5* expression in the developing bud mesenchyme, but (B′,C′) in *hst* mutant embryos, *tbx5* expression is greatly decreased (B′) at 32 hpf and (C′) undetectable in the LPM thereafter. (D-F′) Expression of molecular markers of early limb bud induction. (D,D′) At 32 hpf, wild-type embryos express *shh* expression in the pectoral fin mesenchyme, but *hst* mutant embryos do not. (E,E′) Likewise, at 32 hpf *dlx2* is expressed in the apical fold of wild-type but not *hst* mutant embryos. (F,F′) At 48 hpf, *bmp4* is present in the apical fold of wild-type but not *hst* mutant embryos. (G-I′) *hand2* expression in the developing fin field. (G,G′) At 24 hpf, wild-type embryos express *hand2* broadly in the region of the LPM encompassing the fin field, but *hst* mutant embryos express *hand2* faintly in only a few LPM cells. (H,H′) At 32 and (I,I′) at 48 hfp, wild-type embryos express *hand2* in the fin bud mesenchyme, but *hst* mutant embryos (H′,I′) have no detectable *hand2* expression in the LPM. Arrows in H and G′ indicate cells weakly expressing *hand2*.

Fig. 8. The morphology of *hst* hearts. (A, wild type; B, *hst*) Methylene Blue-stained transverse sections; *hst* hearts have not looped, the atrium is stretched and the ventricle slightly smaller than wild type. a, atrium; i, inflow tract; v, ventricle.

apical epidermis (Fig. 9E,F) (Akimenko et al., 1994; Martinez-Barbera et al., 1997; Neumann et al., 1999). *hst* mutant embryos never express these three markers in the dorsal LPM, although expression of these genes in other regions of the embryo is normal (Fig. 9D′-F′).

The bHLH factor *hand2* normally is expressed in posterior LPM and developing fin (Fig. 9G-I). *hst* mutant embryos show normal *hand2* expression up to the 20-somite stage, greatly reduced expression at 24 hours (Fig. 9G′) and no expression at 32 or 48 hpf (Fig. 9H′,I′). The expression of *hand2* and *tbx5* in the presumptive fin field prior to bud outgrowth suggests that some fin precursor cells differentiate in *hst* mutant embryos, but the buds fail to grow out. Thus, mutation of the *hst* gene reveals an early, essential requirement for Tbx5 in the process of fin field determination or fin bud induction.

Pectoral fins anomalies caused by reduction in Tbx5

The haploinsufficient effects of *tbx5* mutations in human and mouse suggest that Tbx5 functions in the heart and limb are sensitive to dose. Clearly, the zebrafish is not affected by the same degree of Tbx5 deficiency, since *hst* heterozygous fish do not display a mutant phenotype. We progressively lowered levels of Tbx5 in the embryo by varying the concentrations of Tbx5 morpholino injected. Upon injection of 1.7 ng, we observe small pectoral fin buds in about 30% of injected embryos by 48 hpf (Fig. 4E). Although bud growth or initiation is delayed for several hours, all embryos that ultimately develop fins have a morphologically observable bud by 48 hpf.

Delayed buds continue to grow but typically produce abnormal embryonic fins that are shorter along the proximal-distal axis (Fig. 4J,K). Some embryos develop a bud on one side only, and subsequently grow a single fin (Fig. 4K). Some fins develop as stubby appendages, while other fins are overtly normal proximally, but the distal half of the fin folds upwards.

To assess the development of cartilaginous elements that support and shape the fin, we examined histological sections through the developing fins (Fig. 10A-D). Fins of *hst* mutant embryos are shorter, and sometimes severely stunted in growth. Endoskeletal development in fins is often normal proximally,

but defective in the distal up-turned portion (Fig. 10B). In stubby appendages, the endoskeletal disc is several cell layers thick (Fig. 10C,D).

Because of the profound effect of Tbx5 haploinsufficiency in humans and mice (Basson et al., 1994; Bruneau et al., 2001; Newbury-Ecob et al., 1996), we wondered if protracted exposure to this degree of molecular deficiency would elicit fin defects in heterozygous adult fish. Therefore, we examined Alcian Blue/Alizarin Red histological preparations of whole adult pectoral fins (*n*=9 heterozygotes, 9 wild-type controls). We detected no defects in lepidotrichia formation, branching, or attachment of rays to the pectoral girdle at the base of the fin, or in overall fin shape (Fig. 10E,F). Thus, the effects of the *hst* mutation on zebrafish fin formation are fully recessive.
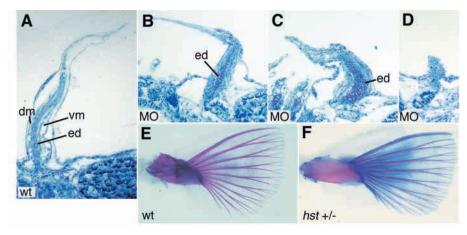
DISCUSSION

The *hst* locus encodes Tbx5

We here report a mutation in the zebrafish *tbx5* ortholog as the cause of the *heartstrings* phenotype. In both the zebrafish *hst* mutant and in human Holt-Oram syndrome, a deficiency of Tbx5 perturbs heart and forelimb development. The cardiac defects of *hst* mutant embryos begin soon after the heart tube formation, as a subtle bradycardia, and progress by 3 dpf to stretching and functional failure of both chambers. The *hst* fin defect is quite pronounced, with failure to develop any molecular or histological evidence of a pectoral fin bud. Phenotypes that perturb fin outgrowth in ways more akin to human haploinsufficiency defects can be elicited by morpholino-induced lowering of the Tbx5 level. This suggests that the dominant nature of the *tbx5* mutation described in humans may reflect a greater sensitivity to Tbx5 level rather than an essential difference in mechanism.

Tbx5 is required for the maturation of cardiac function

Clearly, Tbx5 is essential for normal growth of both chambers of the zebrafish heart. The timing of onset of phenotype well after heart tube formation suggests that the defect does not affect early cardiac progenitors, but rather subsequent growth

Fig. 10. Fin development in morpholino-inhibited buds and in *hst* heterozygous adults. (A-D) Methylene Blue/Azure II-stained transverse sections of pectoral fins at 6 dpf. (A) Wild-type pectoral fin, showing normal development of ventral and dorsal musculature and the endoskeletal disc. (B-D) Pectoral fins of embryos injected with 1.7 ng tbx5-MO show a range of defects, including shortened proximal-distal length and up-turned orientation. (B) Frequently, muscle and endoskeletal disc development appears normal proximally, but is poorly developed in the distal half of the fin. (C) Other fins show greatly thickened endoskeletal disc development or (D) severely stunted growth. (E,F) Pectoral fin

development in *hst* heterozygous adults. (E,F) Alcian Blue/Alizarin Red preparations of adult pectoral fins. Lepidotrichia growth and branching are comparable in (E) wild-type and (F) *hst* heterozygous adults. Fin shapes and sizes are similar. dm, dorsal musculature; ed, endoskeletal disc; vm, ventral musculature.

and differentiation. The specific nature of the cellular pathophysiology remains to be determined.

In humans, the atrium is associated with the most severe and most penetrant aspects of *TBX5* mutation, although defects associated with the ventricle and other areas of the heart have been described (Bruneau et al., 1999; Bruneau et al., 2001; Hatcher et al., 2000a). In mice homozygous for Tbx5 deficiency, sinoatrial structures and the primitive left ventricle are severely hypoplastic (Bruneau et al., 2001). The inflow tract of *hst* mutant embryos appears normal, and cardiac defects include both atrium and ventricle. The particular sensitivity of the atrium in human and mouse may reflect, in part, the *tbx5* expression gradient, which is higher in atrium than ventricle in those species. In the zebrafish, we find that *tbx5* expression extends throughout both chambers, through the initial looping stages. At 48 hpf, the time when deterioration is clearly evident, *tbx5* expression is greater in the ventricle than the atrium, i.e., a pattern reversed relative to other vertebrates.

tbx5 is believed to be important for atrial-ventricular patterning of the heart in other species. In mouse, engineered persistent expression of *tbx5* in the entire heart tube perturbs chamber-specific gene expression and retards ventricular chamber morphogenesis (Liberatore et al., 2000). Overexpression of *tbx5* in cultured human cardiomyocytes inhibits growth and proliferation, suggesting the function of TBX5 is to act as a brake on cellular proliferation (Hatcher and Basson, 2001). Thus, higher expression of *tbx5* in atrial tissues may contribute to their development as thin-walled structures, as opposed to the thick-walled trabecular ventricular chambers (Hatcher and Basson, 2001). However, the expression patterns of markers of early cardiac mesoderm and chamber-specific markers are normal in *hst* mutant embryos, suggesting that the *heartstrings* mutation does not perturb atrial-ventricular patterning in zebrafish. In fact, the predominant cardiac defects of *hst* mutant embryos become evident well after the development of discrete morphological chambers that express chamber-specific markers and after the onset of circulation.

It is of interest, however, that *hst* mutant embryos display an early bradycardia. Pacemaking originates in the sinoatrial region, suggesting that it might be affected as in other species. Bradycardia may be an accompaniment to deficiencies throughout the heart (Warren et al., 2001). Alternatively, Tbx5 could affect the adhesive or conductive properties of cardiomyocytes by regulating the expression of downstream genes such as connexins. In mouse, TBX5 interacts with other transcription factors such as Nkx2.5 to regulate downstream targets with important roles in cardiac growth (ANF) and conduction (Cx40) (Bruneau et al., 2001).

Tbx5 is essential for pectoral fin induction

hst mutant embryos never generate pectoral fin buds, and do not maintain expression of *tbx5* or *hand2* within the differentiating fin field. *hst* mutant embryos do not express markers of the apical fold (*dlx2, bmp4*) or ZPA (*shh*), suggesting fin bud induction is blocked. Thus, the *heartstrings* mutant reveals an essential role for Tbx5 in the earliest stages of bud formation, either in fin bud induction itself or in the determination of the fin field as it coalesces within the lateral plate mesoderm. In other species, FGF10 is a strong candidate for the initial mesoderm-inducing signal. Targeted mutation of *fgf10* or its receptor *FGFR2* in mouse results in a complete or

nearly complete elimination of both fore- and hind-limb buds (Min et el., 1998; Xu et al., 1998; Sekine et al., 1999). Proposed regulators of *fgf10* include *wnt-2b* and *wnt-8c* (Kawakami et al., 2001). Regulatory loops between *Tbx5* and the FGF, WNT and BMP signaling pathways have been proposed (Gibson-Brown et al., 1998; Ohuchi et al., 1998; Rodriguez-Esteban et al., 1999) but the precise relationships are not fully resolved. Once *fgf10* and the relevant *wnts* are cloned in zebrafish, the *hst* mutant can be used to assess the role of Tbx5 in known pathways of limb/fin induction.

Low level inhibition of Tbx5 by morpholino perturbs fin shape, size and endoskeletal development, suggesting an additional role for Tbx5 in coordinating pectoral fin outgrowth. Similarly, in the chick, down-regulation of Tbx5 caused by blockage of FGF signaling in the limb causes loss of the radius and digits (Rodriguez-Esteban et al., 1999). In humans, *tbx5* haploinsufficiency results in forelimb (arm) deformities ranging from subtle abnormalities of the thumb or carpel bones to severe shortening of the arm (OMIM#142900) (Newbury-Ecob et al., 1996). These limb defects in Holt-Oram syndrome are often bilateral but can be asymmetric (Basson et al., 1999). The defects from Tbx5 reduction in the zebrafish also can be asymmetric in severity, suggesting that there may quite sensitive thresholds for effects, as occurs for certain cell fates in response to morphogens (Gurdon and Bourillot, 2001). Alternatively, mosaic distribution of morpholino could account for the asymmetry, but this seems less likely because we injected morpholino into one-celled eggs, and there is no clear left-right allocation of blastomeres to left or right sides in the zebrafish, as is the case in the frog (Abdelilah and Driever, 1997).

The essential elements of many organs, including heart (Kupperman et al., 2000; Rottbauer et al., 2001; Sehnert et al., 2002; Walsh and Stainier, 2001; Xu et al., 2002), blood (Childs et al., 2000; Liao et al., 2002; Lyons et al., 2002), eye (Hutson and Chien, 2002; Malicki et al., 2002; Vihtelic and Hyde, 2002), gut (Allende et al., 1996), kidney (Serluca et al., 2002; Sun and Hopkins, 2001) and bone (Popperl et al., 2000; Schilling et al., 1996) have proved decipherable by zebrafish mutational analysis. The essential genes and their mode of action for normal organ formation clearly are conserved through vertebrate evolution. Similarly, the organotypic elements perturbed in human genetic syndromes are mirrored in the fish with great fidelity.

REFERENCES

Abdelilah, S. and Driever, W. (1997). Pattern formation in *janus*-mutant zebrafish embryos. *Dev. Biol.* **184**, 70-84.

Ahn, D., Kourakis, M. J., Rohde, L. A., Silver, L. M. and Ho, R. K. (2002). T-box gene *tbx5* is essential for formation of the pectoral limb bud. *Nature* **417**, 754-758.

Akimenko, M. A., Ekker, M., Wegner, J., Lin, W. and Westerfield, M. (1994). Combinatorial expression of three zebrafish genes related to *distal-less*: part of a homeobox gene code for the head. *J. Neurosci.* **14**, 3475-3486.

Allende, M. L., Amsterdam, A., Becker, T., Kawakami, K., Gaiano, N. and

Hopkins, N. (1996). Insertional mutagenesis in zebrafish identifies two novel genes, *pescadillo* and *dead eye*, essential for embryonic development. *Genes Dev.* **10**, 3141-3155.

Bamshad, M., Le, T., Watkins, W. S., Dixon, M. E., Kramer, B. E., Roeder, A. D., Carey, J. C., Root, S., Schinzel, A., Van Maldergem, L. et al. (1999). The spectrum of mutations in *TBX3*: Genotype/Phenotype relationship in ulnar-mammary syndrome. *Am. J. Hum. Genet.* **64**, 1550-1562.

Bamshad, M., Lin, R. C., Law, D. J., Watkins, W. C., Krakowiak, P. A., Moore, M. E., Franceschini, P., Lala, R., Holmes, L. B., Gebuhr, T. C. et al. (1997). Mutations in human *TBX3* alter limb, apocrine and genital development in ulnar-mammary syndrome. *Nat. Genet.* **16**, 311-315.

Barresi, M. J., Stickney, H. L. and Devoto, S. H. (2000). The zebrafish *slow-muscle-omitted* gene product is required for Hedgehog signal transduction and the development of slow muscle identity. *Development* **127**, 2189-2199.

Basson, C. T., Bachinsky, D. R., Lin, R. C., Levi, T., Elkins, J. A., Soults, J., Grayzel, D., Kroumpouzou, E., Traill, T. A., Leblanc-Straceski, J. et al. (1997). Mutations in human *TBX5* cause limb and cardiac malformation in Holt-Oram syndrome. *Nat. Genet.* **15**, 30-35.

Basson, C. T., Cowley, G. S., Solomon, S. D., Weissman, B., Poznanski, A. K., Traill, T. A., Seidman, J. G. and Seidman, C. E. (1994). The clinical and genetic spectrum of the Holt-Oram syndrome (heart-hand syndrome). *New Engl. J. Med.* **330**, 885-891.

Basson, C. T., Huang, T., Lin, R. C., Bachinsky, D. R., Weremowicz, S., Vaglio, A., Bruzzone, R., Quadrelli, R., Lerone, M., Romeo, G. et al. (1999). Different *TBX5* interactions in heart and limb defined by Holt-Oram syndrome mutations. *Proc. Natl. Acad. Sci. USA* **96**, 2919-2924.

Begemann, G. and Ingham, P. W. (2000). Developmental regulation of *Tbx5* in zebrafish embryogenesis. *Mech. Dev.* **90**, 299-304.

Begemann, G., Schilling, T. F., Rauch, G. J., Geisler, R. and Ingham, P. W. (2001). The zebrafish *neckless* mutation reveals a requirement for *raldh2* in mesodermal signals that pattern the hindbrain. *Development* **128**, 3081-3094.

Braybrook, C., Doudney, K., Marcano, A. C., Arnason, A., Bjornsson, A., Patton, M. A., Goodfellow, P. J., Moore, G. E. and Stanier, P. (2001). The T-box transcription factor gene *TBX22* is mutated in X-linked cleft palate and ankyloglossia. *Nat. Genet.* **29**, 179-183.

Bruneau, B. G., Logan, M., Davis, N., Levi, T., Tabin, C. J., Seidman, J. G. and Seidman, C. E. (1999). Chamber-specific cardiac expression of *Tbx5* and heart defects in Holt-Oram syndrome. *Dev. Biol.* **211**, 100-108.

Bruneau, B. G., Nemer, G., Schmitt, J. P., Charron, F., Robitaille, L., Caron, S., Conner, D. A., Gessler, M., Nemer, M., Seidman, C. E. et al. (2001). A murine model of Holt-Oram syndrome defines roles of the T-box transcription factor Tbx5 in cardiogenesis and disease. *Cell* **106**, 709-721.

Chapman, D. L., Garvey, N., Hancock, S., Alexiou, M., Agulnik, S. I., Gibson-Brown, J. J., Cebra-Thomas, J., Bollag, R. J., Silver, L. M. and Papaioannou, V. E. (1996). Expression of the T-box family genes, *Tbx1-Tbx5*, during early mouse development. *Dev. Dyn.* **206**, 379-390.

Chen, J. N., van Bebber, F., Goldstein, A. M., Serluca, F. C., Jackson, D., Childs, S., Serbedzija, G. N., Warren, K. S., Mably, J. D., Garrity, D. M. et al. (2001). Genetic steps to organ laterality in zebrafish. *Comp. Funct. Genomics* **2**, 60-68.

Chen, J. N., van Eeden, F. J., Warren, K. S., Chin, A., Nusslein-Volhard, C., Haffter, P. and Fishman, M. C. (1997). Left-right pattern of cardiac *BMP4* may drive asymmetry of the heart in zebrafish. *Development* **124**, 4373-4382.

Childs, S., Weinstein, B. M., Mohideen, M. A., Donohue, S., Bonkovsky, H. and Fishman, M. C. (2000). Zebrafish *dracula* encodes ferrochelatase and its mutation provides a model for erythropoietic protoporphyria. *Curr. Biol.* **10**, 1001-1004.

Christoffels, V. M., Habets, P. E., Franco, D., Campione, M., de Jong, F., Lamers, W. H., Bao, Z. Z., Palmer, S., Biben, C., Harvey, R. P. et al. (2000). Chamber formation and morphogenesis in the developing mammalian heart. *Dev. Biol.* **223**, 266-278.

Dixon, J. W., Costa, T. and Teshima, I. E. (1993). Mosaicism for duplication 12q (12q13→q24.2) in a dysmorphic male infant. *J. Med. Genet.* **30**, 70-72.

Ekker, S. C. and Larson, J. D. (2001). Morphant technology in model developmental systems. *Genesis* **30**, 89-93.

Geisler, R., Rauch, G. J., Baier, H., van Bebber, F., Brobeta, L., Dekens, M. P., Finger, K., Fricke, C., Gates, M. A., Geiger, H. et al. (1999). A radiation hybrid map of the zebrafish genome. *Nat. Genet.* **23**, 86-89.

Ghosh, T. K., Packham, E. A., Bonser, A. J., Robinson, T. E., Cross, S. J. and Brook, J. D. (2001). Characterization of the TBX5 binding site and analysis of mutations that cause Holt-Oram syndrome. *Hum. Mol. Genet.* **10**, 1983-1994.

Gibson-Brown, J. J., Agulnik, S. I., Silver, L. M., Niswander, L. and Papaioannou, V. E. (1998). Involvement of T-box genes *Tbx2-Tbx5* in vertebrate limb specification and development. *Development* **125**, 2499-2509.

Grandel, H. and Schulte-Merker, S. (1998). The development of the paired fins in the zebrafish (Danio rerio). *Mech. Dev.* **79**, 99-120.

Gurdon, J. B. and Bourillot, P. Y. (2001). Morphogen gradient interpretation. *Nature* **413**, 797-803.

Hatcher, C. J. and Basson, C. T. (2001). Getting the T-box dose right. *Nat. Med.* **7**, 1185-1186.

Hatcher, C. J., Goldstein, M. M., Mah, C. S., Delia, C. S. and Basson, C. T. (2000a). Identification and localization of TBX5 transcription factor during human cardiac morphogenesis. *Dev. Dyn.* **219**, 90-95.

Hatcher, C. J., Kim, M. S. and Basson, C. T. (2000b). Atrial form and function: lessons from human molecular genetics. *Trends Cardiovasc. Med.* **10**, 93-101.

Heasman, J. (2002). Morpholino oligos: making sense of antisense? *Dev. Biol.* **243**, 209-214.

Herrmann, B. G. (1991). Expression pattern of the *Brachyury* gene in whole-mount TWis/TWis mutant embryos. *Development* **113**, 913-917.

Hiroi, Y., Kudoh, S., Monzen, K., Ikeda, Y., Yazaki, Y., Nagai, R. and Komuro, I. (2001). Tbx5 associates with Nkx2-5 and synergistically promotes cardiomyocyte differentiation. *Nat. Genet.* **28**, 276-280.

Horb, M. E. and Thomsen, G. H. (1999). *Tbx5* is essential for heart development. *Development* **126**, 1739-1751.

Hutson, L. D. and Chien, C. B. (2002). Pathfinding and error correction by retinal axons: the role of *astray/robo2*. *Neuron* **33**, 205-217.

Imai, Y. and Talbot, W. S. (2001). Morpholino phenocopies of the *bmp2b/swirl* and *bmp7/snailhouse* mutations. *Genesis* **30**, 160-163.

Isaac, A., Rodriguez-Esteban, C., Ryan, A., Altabef, M., Tsukui, T., Patel, K., Tickle, C. and Izpisua-Belmonte, J. C. (1998). *Tbx* genes and limb identity in chick embryo development. *Development* **125**, 1867-1875.

Kawakami, Y., Capdevila, J., Buscher, D., Itoh, T., Rodriguez Esteban, C. and Izpisua Belmonte, J. C. (2001). WNT signals control FGF-dependent limb initiation and AER induction in the chick embryo. *Cell* **104**, 891-900.

Kimmel, C. B., Ballard, W. W., Kimmel, S. R., Ullmann, B. and Schilling, T. F. (1995). Stages of embryonic development of the zebrafish. *Dev. Dyn.* **203**, 253-310.

Knapik, E. W., Goodman, A., Ekker, M., Chevrette, M., Delgado, J., Neuhauss, S., Shimoda, N., Driever, W., Fishman, M. C. and Jacob, H. J. (1998). A microsatellite genetic linkage map for zebrafish (*Danio rerio*). *Nat. Genet.* **18**, 338-343.

Krauss, S., Concordet, J. P. and Ingham, P. W. (1993). A functionally conserved homolog of the Drosophila segment polarity gene *hh* is expressed in tissues with polarizing activity in zebrafish embryos. *Cell* **75**, 1431-1444.

Kupperman, E., An, S., Osborne, N., Waldron, S. and Stainier, D. Y. (2000). A sphingosine-1-phosphate receptor regulates cell migration during vertebrate heart development. *Nature* **406**, 192-195.

Li, Q. Y., Newbury-Ecob, R. A., Terrett, J. A., Wilson, D. I., Curtis, A. R., Yi, C. H., Gebuhr, T., Bullen, P. J., Robson, S. C., Strachan, T. et al. (1997). Holt-Oram syndrome is caused by mutations in *TBX5*, a member of the *Brachyury* (*T*) gene family. *Nat. Genet.* **15**, 21-29.

Liao, E. C., Trede, N. S., Ransom, D., Zapata, A., Kieran, M. and Zon, L. I. (2002). Non-cell autonomous requirement for the *bloodless* gene in primitive hematopoiesis of zebrafish. *Development* **129**, 649-659.

Liberatore, C. M., Searcy-Schrick, R. D. and Yutzey, K. E. (2000). Ventricular expression of *tbx5* inhibits normal heart chamber development. *Dev. Biol.* **223**, 169-180.

Lindsay, E. A., Vitelli, F., Su, H., Morishima, M., Huynh, T., Pramparo, T., Jurecic, V., Ogunrinu, G., Sutherland, H. F., Scambler, P. J. et al. (2001). *Tbx1* haploinsufficieny in the DiGeorge syndrome region causes aortic arch defects in mice. *Nature* **410**, 97-101.

Logan, M., Simon, H. G. and Tabin, C. (1998). Differential regulation of T-box and homeobox transcription factors suggests roles in controlling chick limb-type identity. *Development* **125**, 2825-2835.

Logan, M. and Tabin, C. J. (1999). Role of Pitx1 upstream of Tbx4 in specification of hindlimb identity. *Science* **283**, 1736-1739.

Lyons, S. E., Lawson, N. D., Lei, L., Bennett, P. E., Weinstein, B. M. and Liu, P. P. (2002). A nonsense mutation in zebrafish *gata1* causes the bloodless phenotype in *vlad tepes*. *Proc. Natl. Acad. Sci. USA* **99**, 5454-5459.

Malicki, J. J., Pujic, Z., Thisse, C., Thisse, B. and Wei, X. (2002). Forward

and reverse genetic approaches to the analysis of eye development in zebrafish. *Vision Res.* **42**, 527-533.

Martinez-Barbera, J. P., Toresson, H., Da Rocha, S. and Krauss, S. (1997). Cloning and expression of three members of the zebrafish Bmp family: *Bmp2a*, *Bmp2b* and *Bmp4*. *Gene* **198**, 53-59.

McCorquodale, M. M., Rolf, J., Ruppert, E. S., Kurczynski, T. W. and Kolacki, P. (1986). Duplication (12q) syndrome in female cousins, resulting from maternal (11;12) (p15.5;q24.2) translocations. *Am. J. Med. Genet.* **24**, 613-622.

Melnyk, A. R., Weiss, L., Van Dyke, D. L. and Jarvi, P. (1981). Malformation syndrome of duplication 12q24.1 leads to qter. *Am. J. Med. Genet.* **10**, 357-365.

Merscher, S., Funke, B., Epstein, J. A., Heyer, J., Puech, A., Lu, M. M., Xavier, R. J., Demay, M. B., Russell, R. G., Factor, S. et al. (2001). *TBX1* is responsible for cardiovascular defects in velo-cardio-facial/DiGeorge syndrome. *Cell* **104**, 619-629.

Michelmore, R. W., Paran, I. and Kesseli, R. V. (1991). Identification of markers linked to disease-resistance genes by bulked segregant analysis: a rapid method to detect markers in specific genomic regions by using segregating populations. *Proc. Natl. Acad. Sci. USA* **88**, 9828-9832.

Min, H., Danilenko, D. M., Scully, S. A., Bolon, B., Ring, B. D., Tarpley, J. E., DeRose, M. and Simonet, W. S. (1998). Fgf-10 is required for both limb and lung development and exhibits striking functional similarity to Drosophila *branchless*. *Genes Dev.* **12**, 3156-3161.

Mowbray, C., Hammerschmidt, M. and Whitfield, T. T. (2001). Expression of BMP signalling pathway members in the developing zebrafish inner ear and lateral line. *Mech. Dev.* **108**, 179-184.

Murray, J. C. (2001). Time for T. *Nat. Genet.* **29**, 107-109.

Nagy, E. and Maquat, L. E. (1998). A rule for termination-codon position within intron-containing genes: when nonsense affects RNA abundance. *Trends Biochem. Sci.* **23**, 198-199.

Neumann, C. J., Grandel, H., Gaffield, W., Schulte-Merker, S. and Nusslein-Volhard, C. (1999). Transient establishment of anteroposterior polarity in the zebrafish pectoral fin bud in the absence of sonic hedgehog activity. *Development* **126**, 4817-4826.

Newbury-Ecob, R. A., Leanage, R., Raeburn, J. A. and Young, I. D. (1996). Holt-Oram syndrome: a clinical genetic study. *J. Med. Genet.* **33**, 300-307.

Ohuchi, H., Takeuchi, J., Yoshioka, H., Ishimaru, Y., Ogura, K., Takahashi, N., Ogura, T. and Noji, S. (1998). Correlation of wing-leg identity in ectopic FGF-induced chimeric limbs with the differential expression of chick *Tbx5* and *Tbx4*. *Development* **125**, 51-60.

Popperl, H., Rikhof, H., Chang, H., Haffter, P., Kimmel, C. B. and Moens, C. B. (2000). *lazarus* is a novel *pbx* gene that globally mediates *hox* gene function in zebrafish. *Mol. Cell* **6**, 255-267.

Rodriguez-Esteban, C., Tsukui, T., Yonei, S., Magallon, J., Tamura, K. and Izpisua Belmonte, J. C. (1999). The T-box genes *Tbx4* and *Tbx5* regulate limb outgrowth and identity. *Nature* **398**, 814-818.

Rottbauer, W., Baker, K., Wo, Z. G., Mohideen, M. A., Cantiello, H. F. and Fishman, M. C. (2001). Growth and function of the embryonic heart depend upon the cardiac-specific L-type calcium channel alpha1 subunit. *Dev. Cell* **1**, 265-275.

Ruvinsky, I., Oates, A. C., Silver, L. M. and Ho, R. K. (2000). The evolution of paired appendages in vertebrates: T-box genes in the zebrafish. *Dev. Genes Evol.* **210**, 82-91.

Schilling, T. F., Walker, C. and Kimmel, C. B. (1996). The *chinless* mutation and neural crest cell interactions in zebrafish jaw development. *Development* **122**, 1417-1426.

Sehnert, A. J., Huq, A., Weinstein, B. M., Walker, C., Fishman, M. and Stainier, D. Y. (2002). Cardiac troponin T is essential in sarcomere assembly and cardiac contractility. *Nat. Genet.* **31**, 106-110.

Sekine, K., Ohuchi, H., Fujiwara, M., Yamasaki, M., Yoshizawa, T., Sato, T., Yagishita, N., Matsui, D., Koga, Y., Itoh, N. et al. (1999). Fgf10 is essential for limb and lung formation. *Nat. Genet.* **21**, 138-141.

Serbedzija, G. N., Chen, J. N. and Fishman, M. C. (1998). Regulation in the heart field of zebrafish. *Development* **125**, 1095-1101.

Serluca, F. C., Drummond, I. A. and Fishman, M. C. (2002). Endothelial signaling in kidney morphogenesis. A role for hemodynamic forces. *Curr. Biol.* **12**, 492-497.

Simon, H. (1999). T-box genes and the formation of vertebrate forelimb- and hindlimb specific pattern. *Cell Tissue Res.* **296**, 57-66.

Smith, J. (1999). T-box genes: what they do and how they do it. *Trends Genet.* **15**, 154-158.

Sordino, P., van der Hoeven, F. and Duboule, D. (1995). *Hox* gene expression in teleost fins and the origin of vertebrate digits. *Nature* **375**, 678-681.

Stainier, D. Y. and Fishman, M. C. (1992). Patterning the zebrafish heart tube: acquisition of anteroposterior polarity. *Dev. Biol.* **153**, 91-101.

Sun, Z. and Hopkins, N. (2001). *vhnf1*, the MODY5 and familial GCKD-associated gene, regulates regional specification of the zebrafish gut, pronephros, and hindbrain. *Genes Dev.* **15**, 3217-3229.

Tada, M. and Smith, J. C. (2001). T-targets: clues to understanding the functions of T-box proteins. *Dev. Growth Differ.* **43**, 1-11.

Takeuchi, J. K., Koshiba-Takeuchi, K., Matsumoto, K., Vogel-Hopker, A., Naitoh-Matsuo, M., Ogura, K., Takahashi, N., Yasuda, K. and Ogura, T. (1999). *Tbx5* and *Tbx4* genes determine the wing/leg identity of limb buds. *Nature* **398**, 810-814.

Tamura, K., Kuraishi, R., Saito, D., Masaki, H., Ide, H. and Yonei-Tamura, S. (2001). Evolutionary aspects of positioning and identification of vertebrate limbs. *J. Anat.* **199**, 195-204.

Tamura, K., Yonei-Tamura, S. and Belmonte, J. C. (1999). Differential expression of *Tbx4* and *Tbx5* in zebrafish fin buds. *Mech. Dev.* **87**, 181-184.

Thisse, C., Thisse, B., Schilling, T. F. and Postlethwait, J. H. (1993). Structure of the zebrafish *snail1* gene and its expression in wild-type, *spadetail* and *no tail* mutant embryos. *Development* **119**, 1203-1215.

van Eeden, F. J., Granato, M., Schach, U., Brand, M., Furutani-Seiki, M., Haffter, P., Hammerschmidt, M., Heisenberg, C. P., Jiang, Y. J., Kane, D. A. et al. (1996). Genetic analysis of fin formation in the zebrafish, *Danio rerio*. *Development* **123**, 255-262.

Veitia, R. A. (2002). Exploring the etiology of haploinsufficiency. *BioEssays* **24**, 175-184.

Vihtelic, T. S. and Hyde, D. R. (2002). Zebrafish mutagenesis yields eye morphological mutants with retinal and lens defects. *Vision Res.* **42**, 535-540.

Walsh, E. C. and Stainier, D. Y. (2001). UDP-glucose dehydrogenase required for cardiac valve formation in zebrafish. *Science* **293**, 1670-1673.

Warren, K. S., Baker, K. and Fishman, M. C. (2001). The *slow mo* mutation reduces pacemaker current and heart rate in adult zebrafish. *Am. J. Physiol. Heart Circ. Physiol.* **281**, H1711-1719.

Xu, X., Meiler, S. E., Zhong, T. P., Mohideen, M., Crossley, D. A., Burggren, W. W. and Fishman, M. C. (2002). Cardiomyopathy in zebrafish due to mutation in an alternatively spliced exon of *titin*. *Nat. Genet.* **30**, 205-209.

Xu, X., Weinstein, M., Li, C., Naski, M., Cohen, R. I., Ornitz, D. M., Leder, P. and Deng, C. (1998). Fibroblast growth factor receptor 2 (FGFR2)-mediated reciprocal regulation loop between FGF8 and FGF10 is essential for limb induction. *Development* **125**, 753-765.

Yelon, D., Horne, S. A. and Stainier, D. Y. (1999). Restricted expression of cardiac myosin genes reveals regulated aspects of heart tube assembly in zebrafish. *Dev. Biol.* **214**, 23-37.

Yelon, D. and Stainier, D. Y. (1999). Patterning during organogenesis: genetic analysis of cardiac chamber formation. *Semin. Cell Dev. Biol.* **10**, 93-98.

Yelon, D., Ticho, B., Halpern, M. E., Ruvinsky, I., Ho, R. K., Silver, L. M. and Stainier, D. Y. (2000). The bHLH transcription factor Hand2 plays parallel roles in zebrafish heart and pectoral fin development. *Development* **127**, 2573-2582.